270 *J. Chem. Eng. Data* **1997,** *42,* 270−277

Liquid Densities of Alternative Refrigerants Blended with Difluoromethane, Pentafluoroethane, and 1,1,1,2-Tetrafluoroethane

J. V. Widiatmo,[†] T. Fujimine,* H. Sato, and K. Watanabe

Thermodynamics Laboratory, Department of Mechanical Engineering, Faculty of Science and Technology,
Keio University, 3-14-1, Hiyoshi, Kohoku-ku, Yokohama 223, Japan

---

Measurements of the bubble-point pressures and the saturated-liquid densities of the binary mixtures difluoromethane + 1,1,1,2-tetrafluoroethane (R-32 + R-134a) and pentafluoroethane + 1,1,1,2-tetrafluoroethane (R-125 + R-134a) and the ternary mixture difluoromethane + pentafluoroethane + 1,1,1,2-tetrafluoroethane (R-32 + R-125 + R-134a) are presented. The estimated uncertainties of ±15 mK in temperature, ±12 kPa in pressure, ±0.2% in density, and ±0.3 mol % in composition are reported. The Peng−Robinson equation and the modified Hankinson−Brobst−Thomson equation have been optimized to represent the measured properties satisfactorily. The calculated temperature glides of the mixtures of the present interest have also been presented.

Introduction

Replacement of the conventional refrigerant, chlorodifluoromethane (R-22) is one of the urgent issues to be solved within the scheduled time frame of the amended Montreal Protocol. It is well believed that either a binary or ternary refrigerant mixture constituted by R-32, R-125, and/or R-134a would be the optimum candidate to replace R-22. As a continuation to our previous measurements of thermodynamic properties including the bubble-point pressures and saturated- and compressed-liquid densities (liquid $P\rho Tx$ properties) of the binary R-32 + R-134a and R-32 + R-125 (Widiatmo et al., 1993) systems: similar measurements on the binary R-125 + R-134a system and the ternary R-32 + R-125 + R-134a system are reported here along with an evaluation of reliable representations of bubble-point pressures and saturated-liquid densities for industrial applications.

Experimental Apparatus

All measurements in the present work were performed with a magnetic densimeter coupled with a variable volume cell which enables measurements either at the saturated-liquid condition or at the compressed-liquid condition. The saturation state of the mixture of the known composition was determined by observing the appearance and disappearance of a bubble in the liquid phase. Since the details of the apparatus have been reported elsewhere (Widiatmo et al., 1993), it will not be repeated in the present paper. By using the present apparatus, the bubble-point pressures were determined with uncertainties within ±12 kPa, while the densities were within ±0.2%. The uncertainty of temperature and pressure measurements were estimated to be within ±15 mK and ±12 kPa, respectively, while the determination of the composition of the mixture was done within ±0.3 mol %. The purity of the samples analyzed by the manufacturers was 99.998 mass % for R-32, 99.98 mass % for R-125, and 99.8 mass % for R-134a, respectively, and no further purification was performed in the present work.

Results and Discussion

Table 1. Bubble-Point Pressures of R-125 (1) + R-134a (2)

x_1	T/K	P/MPa	x_1	T/K	P/MPa
0.0866	279.988	0.425	0.4603	299.987	1.065
0.0866	289.987	0.580	0.4603	309.986	1.372
0.0866	299.987	0.790			
0.0866	309.987	1.025	0.6653	279.988	0.684
0.0866	319.986	1.324	0.6653	289.987	0.919
0.0866	329.986	1.692	0.6653	299.987	1.200
0.0866	339.985	2.144	0.6653	309.987	1.549
0.0866	349.984	2.635	0.6653	319.987	1.976
			0.6653	329.986	2.506
0.2674	279.988	0.512			
0.2674	289.987	0.685	0.9231	279.988	0.792
0.2674	299.987	0.912	0.9231	289.987	1.078
0.2674	309.988	1.193	0.9231	299.987	1.405
0.2674	319.986	1.524	0.9231	309.987	1.802
0.2674	329.986	1.946	0.9231	319.987	2.280
0.2674	339.985	2.410	0.9231	329.986	2.886
0.2674	349.984	2.973	0.9231	319.986	2.269
			0.9231	329.986	2.870
0.4603	279.988	0.600			
0.4603	289.987	0.807			
0.4603	309.987	1.382			
0.4603	329.987	2.239			

The bubble-point pressures and saturated- and compressed-liquid densities of the binary R-32 + R-134a system are obtained only for compositions of 20, 25, 40, 60, and 80 mass % R-32 (0.3293, 0.3953, 0.5661, 0.7483, and 0.8869 mole fraction of R-32). Those of the binary R-125 + R-134a system are measured for temperatures from 280 to 350 K in 10 K intervals and for compositions of 10, 30, 50, 70, and 93 mass % R-125 (0.0866, 0.2674, 0.4603, 0.6653, and 0.9231 mole fraction of R-125), while those of the ternary R-32 + R-125 + R-134a system for compositions of 20/40/40 (0.3470/0.2994/0.3536 mole fraction), 23/25/52 (0.3819/0.1792/0.4389 mole fraction), and 30/10/60 mass % (0.4639/0.0699/0.4662 mole fraction). The first two compositions of the ternary system are already designated by the ASHRAE (American Society of Heating, Refrigerating and Air-conditioning Engineers) as R-407A and R-407C, respectively, and are considered to be the promising alternatives to R-22. The numerical bubble-point pressure and saturated- and compressed-liquid density data of this work for all three systems are listed in Tables 1−9.

The measured bubble-point pressures of the binary and ternary systems composed of R-32, R-125, and R-134a are summarized by a three-dimensional plot shown in Figure 1, while the saturated-liquid molar volumes are illustrated in Figure 2. The abscissa denotes the mole fraction of each

---

* To whom correspondence should be addressed.

[†] Agency for the Assessment and Application of Technology, Republic of Indonesia.

S0021-9568(96)00232-4 CCC: $14.00

Table 2. Saturated-Liquid Densities of R-125 (1) + R-134a (2)

x_1	T/K	ρ/kg·m^{-3}	x_1	T/K	ρ/kg·m^{-3}
0.0866	279.988	1276.3	0.4603	319.987	1095.2
0.0866	289.987	1240.5	0.4603	329.987	1028.2
0.0866	299.987	1202.0	0.4603	339.984	954.8
0.0866	309.987	1160.7	0.4603	299.987	1201.3
0.0866	319.986	1115.1	0.4603	309.986	1151.4
0.0866	329.986	1065.2			
0.0866	339.985	1008.4	0.6653	279.988	1289.1
0.0866	349.984	938.0	0.6653	289.987	1244.2
			0.6653	299.988	1195.6
0.2674	279.988	1282.6	0.6653	309.987	1141.1
0.2674	289.987	1244.3	0.6653	319.987	1079.0
0.2674	299.988	1202.6	0.6653	329.986	1003.4
0.2674	309.987	1158.9			
0.2674	319.986	1109.3	0.9231	279.988	1288.7
0.2674	329.986	1053.0	0.9231	289.987	1239.8
0.2674	339.985	986.5	0.9231	299.987	1185.5
0.2674	349.984	901.8	0.9231	309.987	1117.7
			0.9231	319.987	1043.0
0.4603	279.988	1286.5	0.9231	329.986	950.0
0.4603	309.987	1151.6	0.9231	319.986	1045.1
0.4603	289.987	1245.1	0.9231	329.986	948.7
0.4603	299.987	1201.3			

component, and the ordinate shows the properties of the pure components (R-32, R-125, and R-134a), the binary (R-32 + R-125, R-32 + R-134a, and R-125 + R-134a) systems, and the ternary (R-32 + R-125 + R-134a) system. The surface surrounded by the triangle representing the properties of the binary mixtures corresponds to the properties of the ternary system at each temperature. The solid lines in Figure 1 are calculated from the Peng−Robinson (PR) equation (Peng and Robinson, 1976) with the binary interaction parameters determined exclusively based on the present measurements. The PR equation has a functional form given by

$$P = \frac{RT}{(v - b)} - \frac{a}{v(v + b) + b(v - b)} \tag{1}$$

$$a = 0.45724\alpha R^2 T_c/P_c \tag{2}$$

$$b = 0.07780 R T_c/P_c \tag{3}$$

$$a = [1 + (0.37464 + 1.54226\omega - 0.26992\omega^2)(1 - \sqrt{T/T_c})]^2 \tag{4}$$

$$\omega = -\log(P^{\Phi}/P_c) \tag{5}$$

where P^{Φ} is the vapor pressure at $0.7T_c$.

The proposed mixing rules are given as follows:

$$a_m = \sum_i \sum_j x_i x_j (1 - k_{ij})\sqrt{a_i a_j} \tag{6}$$

$$b_m = \sum_i x_i b_i \tag{7}$$

The k_{ij} in eq 6 is known as the binary interaction parameter for the binary mixtures. It is clear from eqs 1−5 that the critical temperature, T_c, critical pressure P_c, and the acentric factor, ω, are required to apply the PR equation. Application of the PR equation to mixtures is easily performed whenever the information about the required parameters aforementioned of each component is known. The parameters appearing in eqs 1−7 are listed for HFC refrigerants of the present interest in Table 10.

The plotted pure component data in Figure 1 are those by Widiatmo et al. (1994) for R-32 and R-125 and the calculated values from the equation of state by Piao et al. (1990) for R-134a, while the binary R-32 + R-125 system data are those by Widiatmo et al. (1993). The other data for the binary R-125 + R-134a and R-32 + R-134a and the ternary R-32 + R-125 + R-134a systems are the present results. As shown in Figure 1, the binary R-125 + R-134a and R-32 + R-134a systems are zeotropic blends, while the binary R-32 + R-125 system is an azeotropic one. The dashed lines show the calculated dew-point pressures from the PR equation. The thin solid lines are isotherms for the bubble-point pressures of the ternary R-32 + R-125 + R-134a system at a mole fraction of 0.3536 of R-134a (corresponds to 20/40/40 mass % R-32 + R-125 + R-134a), at 0.4388 of R-134a (corresponds to 23/25/52 mass % R-32 + R-125 + R-134a), and at 0.4692 of R-134a (corresponds to 30/10/60 mass % R-32 + R-125 + R-134a), which are also calculated from the PR equation by simply introducing the binary interaction parameters of its corresponding binary systems. Such a representation may provide a little complicated view of the bubble-point pressure surface of the ternary system because of an inclusion of the isotherms. However, it would be useful to overview general behaviors of the bubble-point pressures of the single-component, the binary, and the ternary systems.

The solid lines in Figure 2 are calculated from the modified Hankinson−Brobst−Thomson (HBT) equation proposed by Maezawa et al. (1993), which also requires the binary interaction parameters. The modified HBT equation has the functional form given below:

$$v_{s,m} = v^*_m v_R^{(0)}(1 - \omega_m v_R^{(\delta)}) \tag{8}$$

where

$$v_R^{(0)} = 1 + a\tau^{1/3} + b\tau^{2/3} + c\tau + d\tau^{4/3} \tag{9}$$

$$v_R^{(\delta)} = \frac{e + fT_R + gT_R^{\,2} + hT_R^{\,3}}{T_R - 1.00001} \tag{10}$$

and

$$\tau = 1 - T/T_{c,m} \qquad T_R = T/T_{c,m} \tag{11}$$

In the above expressions, the subscripts R and m denote nondimensional reduced values to the critical point values and mixture, respectively. Namely, $v_{s,m}$ is the saturated-liquid molar volume of the mixture and $T_{c,m}$ denotes the critical temperature of the mixture given by the following equation.

$$T_{c,m} = \sum_i \sum_j x_i x_j (1 - k_{ij})\sqrt{v^*{}_i T_{c,i} v^*{}_j T_{c,jj}}/v^*{}_m \tag{12}$$

where

$$v^*{}_m = [\sum_i \sum_i x_i v^*_i + 3(\sum_i x v_i^{*1/3})(\sum_i x_i v_i^{*2/3})]/4 \tag{13}$$

$$\omega_m = \sum_i \sum_j x_i x_j (1 - l_{ij})\sqrt{\omega_i \omega_j} \tag{14}$$

$$\omega = -\log(P^{\Phi}/P_c) \tag{15}$$

where P^{Φ} is the vapor pressure at $0.7T_c$. The parameter values for each constituent used in the present modified HBT equation are listed in Table 10, whereas the numerical constants a through h appearing in eqs 9 and 10 are given below: $a = -1.528\,16$, $b = 1.439\,07$, $c = -0.814\,46$,

Table 3. Liquid $PVTx$ Properties of R-125 (1) + R-134a (2)

x_1	T/K	P/MPa	ρ/kg·m^{-3}	x_1	T/K	P/MPa	ρ/kg·m^{-3}
0.0866[a]	279.988	0.425	1276.3	0.0866	309.987	1.506	1164.2
0.0866	279.988	1.001	1278.5	0.0866	309.987	2.005	1168.2
0.0866	279.988	1.503	1280.4	0.0866	309.987	2.507	1172.1
0.0866	279.988	2.002	1282.9	0.0866	309.986	3.007	1175.9
0.0866	279.988	2.499	1284.9	0.0866[a]	319.986	1.324	1115.1
0.0866	279.988	3.012	1286.5	0.0866	319.986	1.508	1117.2
0.0866[a]	289.987	0.580	1240.5	0.0866	319.986	2.005	1122.4
0.0866	289.987	1.005	1242.3	0.0866	319.986	2.505	1127.4
0.0866	289.987	1.507	1244.6	0.0866	319.986	2.996	1132.1
0.0866	289.987	2.005	1247.5	0.0866[a]	329.986	1.692	1065.2
0.0866	289.987	2.504	1249.8	0.0866	329.987	2.009	1069.9
0.0866	289.987	3.004	1252.0	0.0866	329.986	2.510	1076.7
0.0866[a]	299.987	0.790	1202.0	0.0866	329.986	3.008	1083.1
0.0866	299.987	1.009	1203.5	0.0866[a]	339.985	2.144	1008.4
0.0866	299.987	1.510	1207.0	0.0866	339.985	2.510	1016.0
0.0866	299.987	2.009	1210.0	0.0866	339.985	3.005	1025.4
0.0866	299.987	2.502	1213.2	0.0866[a]	349.984	2.635	938.0
0.0866	299.987	3.004	1216.2	0.0866	349.985	3.004	950.8
0.0866[a]	309.987	1.025	1160.7				
0.2674	299.987	3.011	1218.7	0.2674[a]	279.988	0.512	1282.6
0.2674[a]	309.987	1.193	1158.9	0.2674	279.988	1.003	1285.0
0.2674	309.987	1.508	1162.0	0.2674	279.988	1.506	1287.5
0.2674	309.987	2.010	1166.8	0.2674	279.988	2.012	1290.1
0.2674	309.986	2.513	1171.5	0.2674	279.988	2.510	1291.8
0.2674	309.986	3.006	1175.7	0.2674	279.988	3.007	1293.8
0.2674[a]	319.986	1.524	1109.3	0.2674[a]	289.987	0.685	1244.3
0.2674	319.987	2.010	1115.7	0.2674	289.987	1.010	1246.2
0.2674	319.986	2.507	1121.9	0.2674	289.987	1.501	1249.1
0.2674	319.987	3.003	1127.6	0.2674	289.987	2.010	1252.2
0.2674[a]	329.986	1.946	1053.0	0.2674	289.987	2.509	1254.9
0.2674	329.986	2.507	1062.9	0.2674	289.987	3.004	1257.6
0.2674	329.986	3.012	1070.7	0.2674[a]	299.987	0.912	1202.6
0.2674[a]	339.985	2.410	986.5	0.2674	299.987	1.510	1207.4
0.2674	339.985	2.999	1002.9	0.2674	299.987	2.009	1211.5
0.2674[a]	349.984	2.973	901.8	0.2674	299.987	2.506	1214.9
0.4603[a]	279.988	0.600	1286.5	0.4603	309.986	1.492	1152.9
0.4603	279.988	1.009	1289.1	0.4603	309.987	2.007	1159.1
0.4603	279.988	1.505	1291.8	0.4603	309.987	2.514	1164.8
0.4603	279.988	2.011	1294.6	0.4603	309.987	3.009	1170.3
0.4603	279.988	2.505	1297.2	0.4603[a]	319.987	1.758	1095.2
0.4603	279.988	3.016	1299.9	0.4603	319.987	1.844	1095.2
0.4603[a]	289.987	0.807	1245.1	0.4603	319.986	2.014	1097.9
0.4603	289.987	1.001	1247.0	0.4603	319.986	2.523	1105.7
0.4603	289.987	1.513	1250.7	0.4603	319.986	3.014	1113.1
0.4603	289.987	2.007	1254.4	0.4603[a]	329.987	2.239	1028.2
0.4603	289.987	2.502	1257.9	0.4603	329.986	2.504	1037.5
0.4603	289.987	3.014	1261.1	0.4603	329.986	3.017	1049.8
0.4603[a]	299.987	1.114	1201.3	0.4603[a]	339.984	2.798	954.8
0.4603	299.987	1.509	1204.9	0.4603	339.984	2.863	954.8
0.4603	299.987	2.002	1209.3	0.4603	339.985	3.010	961.8
0.4603	299.988	2.505	1213.5	0.4603[a]	299.987	1.065	1201.3
0.4603	299.988	3.009	1217.8	0.4603[a]	309.986	1.372	1151.4
0.4603[a]	309.988	1.382	1151.6				
0.6653[a]	279.988	0.652	1289.9	0.6653	289.987	1.500	1251.4
0.6653	279.988	1.015	1292.4	0.6653	289.987	2.009	1255.4
0.6653	279.988	1.510	1295.3	0.6653	289.987	2.503	1259.0
0.6653	279.988	2.026	1298.7	0.6653	289.987	3.004	1262.8
0.6653	279.988	2.515	1301.6	0.6653[a]	299.987	1.168	1198.8
0.6653	279.988	3.007	1304.4	0.6653	299.987	1.504	1202.6
0.6653[a]	289.987	0.874	1246.1	0.6653	299.987	2.008	1207.3
0.6653	289.987	1.014	1247.4	0.6653	299.987	2.503	1212.3
0.9231[a]	279.988	0.792	1288.7	0.9231	299.987	1.504	1186.5
0.9231	279.988	1.008	1290.5	0.9231	299.987	1.993	1194.0
0.9231	279.988	1.508	1294.5	0.9231	299.987	2.513	1201.0
0.9231	279.988	2.004	1298.6	0.9231	299.988	3.002	1207.2
0.9231	279.988	2.504	1302.4	0.9231[a]	309.988	1.802	1117.7
0.9231	279.988	3.008	1306.1	0.9231	309.986	2.006	1122.3
0.9231[a]	289.987	1.078	1239.8	0.9231	309.986	2.502	1133.0
0.9231	289.987	1.506	1244.3	0.9231	309.987	3.003	1142.8
0.9231	289.987	2.005	1249.4	0.9231[a]	319.986	2.269	1043.1
0.9231	289.987	2.506	1254.1	0.9231[a]	319.987	2.280	1043.0
0.9231	289.987	3.008	1258.8	0.9231	319.987	2.504	1054.0
0.9231[a]	299.987	1.405	1185.5	0.9231	319.987	3.004	1070.4

[a] Two phase condition.

Table 4. Bubble-Point Pressures of R-32 (1) + R-134a (2)

x_1	T/K	P/MPa	x_1	T/K	P/MPa
0.3293	279.987	0.577	0.5667	229.974	0.110
0.3293	289.986	0.783	0.5667	239.977	0.170
0.3293	299.986	1.052	0.5667	249.980	0.261
0.3293	329.984	2.226	0.5667	259.882	0.373
0.3291	309.985	1.407	0.5667	269.987	0.531
0.3291	319.985	1.752			
0.3291	339.983	2.747	0.7460	279.988	0.859
			0.7460	289.989	1.133
0.3955	219.971	0.056	0.7460	299.988	1.489
0.3955	229.975	0.091	0.7460	299.987	1.489
0.3955	234.976	0.114	0.7460	309.986	1.923
0.3955	239.977	0.142	0.7460	309.986	1.923
0.3955	249.980	0.217	0.7460	309.986	1.923
0.3955	259.983	0.315	0.7460	319.985	2.446
0.3955	269.980	0.460	0.7483	279.986	0.855
0.3953	279.999	0.629	0.7483	289.987	1.147
0.3953	290.000	0.840	0.7483	299.985	1.514
0.3953	300.000	1.111	0.7483	309.985	1.944
0.3953	309.999	1.443	0.7483	319.985	2.475
0.3953	320.000	1.858	0.7483	329.987	3.095
0.3953	330.000	2.344			
0.5661	279.988	0.764			
0.5661	289.987	1.005	0.8869	279.988	0.942
0.5661	299.986	1.309	0.8869	289.988	1.264
0.5661	309.985	1.689	0.8869	299.986	1.657
0.5661	319.985	2.196	0.8869	309.985	2.142
0.5661	329.984	2.712	0.8869	319.985	2.715
0.5667	219.970	0.069			

Table 5. Saturated-Liquid Densities of R-32 (1) + R-134a (2)

x_1	T/K	ρ/kg·m^{-3}	x_1	T/K	ρ/kg·m^{-3}
0.3293	279.987	1213.6	0.8869	279.988	1070.3
0.3293	289.986	1177.2	0.8869	289.988	1031.4
0.3293	299.986	1141.6	0.8869	299.986	996.1
0.3293	329.984	999.9	0.8869	309.985	951.1
0.3291	309.985	1100.8	0.8869	319.985	897.1
0.3291	319.985	1053.2			
0.3291	339.983	940.7	0.7483	279.986	1113.4
			0.7483	289.987	1075.1
0.3953	279.999	1196.9	0.7483	299.985	1040.1
0.3953	290.000	1162.1	0.7483	309.985	997.4
0.3953	300.000	1124.2	0.7483	319.985	944.8
0.3953	309.999	1081.9	0.7483	329.987	884.8
0.3953	320.000	1036.7			
0.3953	330.000	982.8	0.7460	279.988	1115.0
0.3955	219.971	1387.3	0.7460	289.989	1077.9
0.3955	229.975	1358.1	0.7460	299.987	1037.8
0.3955	234.976	1344.3	0.7460	299.988	1039.2
0.3955	239.977	1329.1	0.7460	309.986	992.3
0.3955	249.980	1299.4	0.7460	319.985	948.3
0.3955	259.983	1266.0			
0.3955	269.987	1233.5			
0.5661	279.988	1160.1			
0.5661	289.987	1121.1			
0.5661	299.986	1083.9			
0.5661	309.985	1040.0			
0.5661	319.985	996.9			
0.5661	329.984	938.8			

Table 6. Liquid *PVTx* Properties of R-32 (1) + R-134a (2)

x_1	T/K	P/MPa	ρ/kg·m^{-3}	x_1	T/K	P/MPa	ρ/kg·m^{-3}
0.3955	249.980	0.502	1299.2	0.3953	279.999	3.000	1206.5
0.3955	249.981	1.009	1300.6	0.3953	290.001	1.000	1163.0
0.3955	249.981	1.503	1301.4	0.3953	290.000	1.501	1165.7
0.3955	249.981	2.002	1302.9	0.3953	290.000	2.002	1168.4
0.3955	259.984	0.511	1267.9	0.3953	290.000	2.505	1170.9
0.3955	259.986	1.036	1269.1	0.3953	290.000	3.002	1173.4
0.3955	259.986	1.504	1270.6	0.3953	300.000	1.505	1126.5
0.3955	259.984	2.022	1272.8	0.3953	300.000	2.005	1129.7
0.3955	269.986	0.545	1233.4	0.3953	300.000	2.501	1133.1
0.3955	269.986	1.001	1235.1	0.3953	300.000	3.001	1136.0
0.3955	269.987	1.500	1236.3	0.3953	310.000	2.001	1086.8
0.3955	269.989	2.011	1238.6	0.3953	310.000	2.526	1092.7
0.3955	269.987	2.503	1241.2	0.3953	310.000	3.006	1097.1
0.3955	269.987	3.005	1242.7	0.3953	320.000	2.004	1038.5
0.3953	280.000	1.002	1198.5	0.3953	320.000	2.503	1043.7
0.3953	280.000	1.502	1200.6	0.3953	320.000	2.999	1048.8
0.3953	280.000	2.004	1202.7	0.3953	330.001	2.507	985.7
0.3953	280.000	2.501	1204.6	0.3953	300.001	3.002	993.1

Table 7. Bubble-Point Pressures of R-32 (1) + R-125 (2) + R-134a (3)

x_1	x_2	T/K	P/MPa	x_1	x_2	T/K	P/MPa
0.3470	0.2994	279.988	0.767	0.3819	0.1792	319.986	2.079
0.3470	0.2994	289.989	1.012	0.3819	0.1792	329.985	2.608
0.3470	0.2994	299.987	1.325	0.3819	0.1792	339.985	3.241
0.3470	0.2294	309.986	1.712				
0.3470	0.2994	319.986	2.172	0.4639	0.0669	289.987	0.954
0.3470	0.2994	329.987	2.718	0.4639	0.0669	299.987	1.253
				0.4639	0.0669	299.987	1.254
0.3819	0.1792	279.988	0.724	0.4639	0.0669	309.987	1.619
0.3819	0.1792	289.987	0.948	0.4639	0.0669	309.987	1.621
0.3819	0.1792	289.986	0.947	0.4639	0.0669	319.986	2.060
0.3819	0.1792	299.987	1.250				
0.3819	0.1792	309.987	1.618				

Table 8. Saturated-Liquid Densities of R-32 (1) + R-125 (2) + R-134a (3)

x_1	x_2	T/K	ρ/kg·m^{-3}	x_1	x_2	T/K	ρ/kg·m^{-3}
0.3470	0.2994	279.988	1221.2	0.3819	0.1792	339.985	896.6
0.3470	0.2994	289.989	1179.4				
0.3470	0.2994	299.987	1133.1	0.4639	0.0669	279.988	1186.3
0.3470	0.2994	309.986	1084.0	0.4639	0.0669	279.988	1186.3
0.3470	0.2994	319.986	1027.9	0.4639	0.0669	289.987	1148.6
0.3470	0.2994	329.987	962.8	0.4639	0.0669	299.987	1108.6
				0.4639	0.0669	299.987	1107.2
0.3819	0.1792	279.988	1210.1	0.4639	0.0669	299.987	1107.6
0.3819	0.1792	289.987	1170.5	0.4639	0.0669	309.987	1063.4
0.3819	0.1792	289.986	1170.7	0.4639	0.0669	309.987	1063.6
0.3819	0.1792	299.987	1128.8	0.4639	0.0669	319.986	1014.5
0.3819	0.1792	309.987	1082.5				
0.3819	0.1792	319.986	1027.5				
0.3819	0.1792	329.985	968.0				

$d = 0.190\,454$, $e = -0.296\,123$, $f = 0.386\,914$, $g = -0.042\,725\,8$, $h = -0.048\,064\,5$.

k_{ij} and l_{ij}, binary interaction parameters in eqs 12 and 14, are introduced by Maezawa et al. (1993) to make necessary modification to the critical temperature, $T_{c,m}$, acentric factor, ω_m, and critical locus. These binary parameters are optimized on the basis of the measured saturated-liquid densities. k_{ij} and l_{ij} for the binary R-32 + R-134a, R-32 + R-125, and R-125 + R-134a systems are listed in Table 11.

The solid line for the binary R-32 + R-125 system at 340 K does not intersect with the ordinate for R-125 in Figure 2, since this 340 K isotherm becomes a supercritical isotherm (note that the critical temperature of R-125 is 339.17 K (Ikeda et al., 1994)). The same tendency also appears for the solid line of the 340 K isotherm for the binary R-125 + R-134a system. The thin solid lines in Figure 2 are calculated from the modified HBT equation by simply employing the binary interaction parameters of the corresponding binary systems. The plotted pure component data are those by Widiatmo et al. (1994) for R-32 and R-125 and by Maezawa et al. (1990) for R-134a, while the binary R-32 + R-125 system data are those by Widiatmo et al. (1993). The other data for the binary R-125 + R-134a and R-32 + R-134a and the ternary R-32 + R-125 + R-134a systems are the present results.

The PR equation requires an optimization of the binary interaction parameter on the basis of the measured data when it is applied to the mixtures. In this work, the binary

Table 9. Liquid *PVTx* Properties of R-32 (1) + R-125 (2) + R-134a (3)

x_1	x_2	T/K	P/MPa	ρ/kg·m^{-3}	x_1	x_2	T/K	P/MPa	ρ/kg·m^{-3}
0.3819[a]	0.1792	279.988	0.724	1210.1	0.4639[a]	0.0669	279.988	0.730	1186.3
0.3819	0.1792	279.988	1.001	1211.4	0.4639[a]	0.0669	279.988	0.739	1186.3
0.3819	0.1792	279.988	1.501	1214.0	0.4639[a]	0.0669	279.988	1.001	1187.6
0.3819	0.1792	279.988	2.001	1216.3	0.4639	0.0669	279.988	1.500	1189.0
0.3819	0.1792	279.988	2.500	1218.5	0.4639	0.0669	279.988	2.002	1191.3
0.3819	0.1792	279.988	3.001	1220.4	0.4639	0.0669	279.988	2.501	1192.8
0.3819[a]	0.1792	289.987	0.948	1170.5	0.4639	0.0669	279.988	3.001	1195.2
0.3819[a]	0.1792	289.986	0.947	1170.7	0.4639[a]	0.0669	289.987	0.954	1148.6
0.3819	0.1792	289.987	1.001	1171.3	0.4639	0.0669	289.987	1.001	1149.1
0.3819	0.1792	289.986	1.502	1174.4	0.4639	0.0669	289.988	1.501	1150.5
0.3819	0.1792	289.987	2.002	1177.4	0.4639	0.0669	289.987	2.001	1153.3
0.3819	0.1792	289.987	2.501	1180.4	0.4639	0.0669	289.987	2.501	1155.9
0.3819	0.1792	289.987	3.001	1183.3	0.4639	0.0669	289.987	3.002	1158.5
0.3819[a]	0.1792	299.987	1.250	1128.8	0.4639[a]	0.0669	299.987	1.253	1107.2
0.3819	0.1792	299.987	1.502	1130.6	0.4639[a]	0.0669	299.987	1.254	1107.6
0.3819	0.1792	299.987	2.002	1134.4	0.4639	0.0669	299.987	1.278	1108.6
0.3819	0.1792	299.987	2.501	1138.2	0.4639	0.0669	299.987	1.502	1109.2
0.3819	0.1792	299.987	3.002	1141.9	0.4639	0.0669	299.987	2.002	1112.9
0.3819[a]	0.1792	309.987	1.618	1082.5	0.4639	0.0669	299.987	2.501	1116.3
0.3819	0.1792	309.987	2.003	1086.5	0.4639	0.0669	299.987	3.001	1119.5
0.3819	0.1792	309.987	2.502	1091.5	0.4639[a]	0.0669	309.987	1.619	1063.4
0.3819[a]	0.1792	319.986	2.079	1027.5	0.4639[a]	0.0669	309.987	1.621	1063.6
0.3819	0.1792	319.986	2.503	1033.9	0.4639	0.0669	309.987	2.002	1066.6
0.3819	0.1792	319.986	3.002	1045.8	0.4639	0.0669	309.987	2.501	1071.2
0.3819[a]	0.1792	329.985	2.608	968.0	0.4639	0.0669	309.987	3.002	1075.3
0.3819	0.1792	329.985	3.007	976.7	0.4639[a]	0.0669	319.987	2.060	1014.5
0.3819[a]	0.1792	339.985	3.241	896.6					

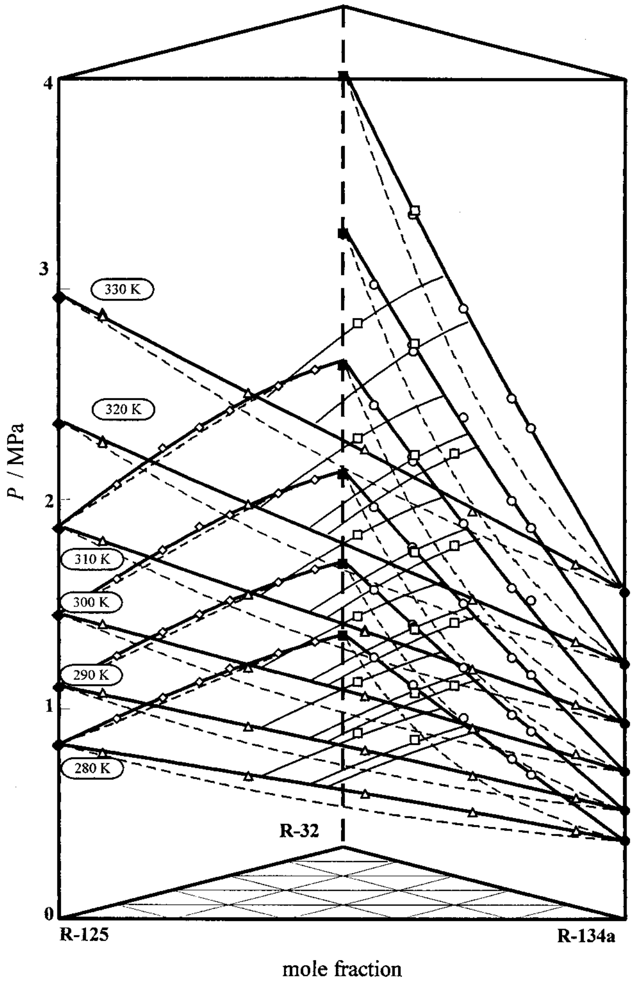

Figure 1. Bubble-point pressures of mixtures blended with R-32, R-125, and R-134a: (○) this work (R-32 + R-134a); (◇) Widiatmo (R-32 + R-125); (△) this work (R-125 + R-134a); (□) this work (R-32 + R-125 + R-134a); (■) Widiatmo (R-32); (◆) Widiatmo (R-125); (●) Piao (R-134a).

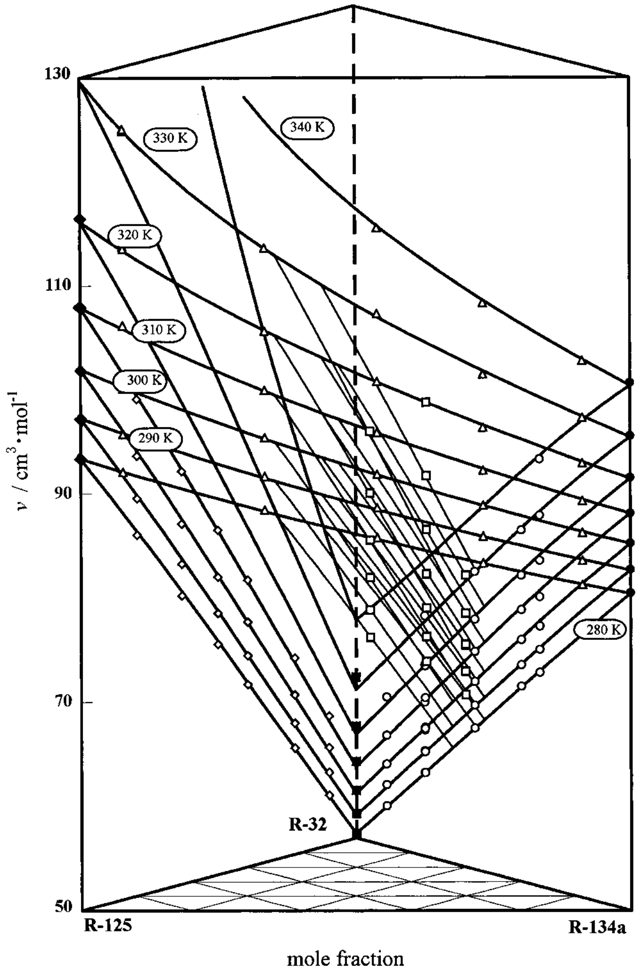

Figure 2. Saturated-liquid molar volumes of mixtures blended with R-32, R-125, and R-134a: (○) this work (R-32 + R-134a); (◇) Widiatmo (R-32 + R-125); (△) this work (R-125 + R-134a); (□) this work (R-32 + R-125 + R-134a); (■) Widiatmo (R-32); (◆) Widiatmo (R-125); (●) Maezawa (R-134a).

interaction parameter is optimized only by fitting the PR equation to the bubble-point pressure data. The available bubble-point pressure data of the binary R-32 + R-134a system besides the present measurements are those by

Table 10. Parameters Used in the PR and Modified HBT Equations

	R-32	R-125	R-134a
T_c/K	351.26[a]	339.17[b]	374.11[a]
P_c/MPa	5.780[c]	3.620[d]	4.064[e]
ρ_c/kg·m^{-3}	427[a]	577[b]	508[a]
M	52.024	120.02	102.031
ω	0.277	0.305	0.327
v^*/cm^3·mol^{-1}	116.8	209.8	198.0

[a] Higashi (1995a). [b] Ikeda et al. (1994). [c] Qian et al. (1993). [d] Sagawa et al. (1994). [e] Piao et al. (1990).

Table 11. Binary Interaction Parameters of the Modified HBT Equation

system	k_{ij}	l_{ij} (T in K)
R-32 + R-134a	−0.009	$l_{ij} = 5.17 \times 10^{-5}T^2 - 2.33 \times 10^{-2}T + 2.78$
R-32 + R-125	0	0.50
R-125 + R-134a	−0.003	$l_{ij} = 1.32 \times 10^{-4}T^2 - 7.45 \times 10^{-2}T + 10.48$

Table 12. Binary Interaction Parameters of the PR Equation

system	k_{ij} (T in K)
R-32 + R-134a	$k_{ij} = 3.96 \times 10^{-5}T - 8.05 \times 10^{-14}T^{4.5}$
R-32 + R-125	$k_{ij} = -4.66 \times 10^{-2} + 1.69 \times 10^{-4}T$
R-125 + R-134a	$k_{ij} = 5.74 \times 10^{-2} - 1.60 \times 10^{-4}T$

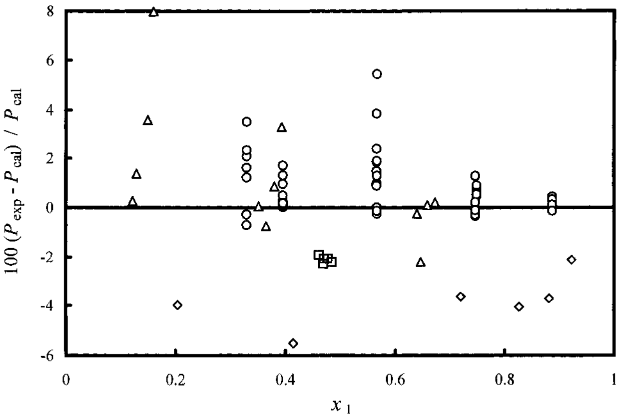

Figure 3. Bubble-point pressure divation from the PR equation for the binary R-32 + R-134a system: (◇) Fujiwara; (△) Higashi; (○) this work; (□) Kleemiss.

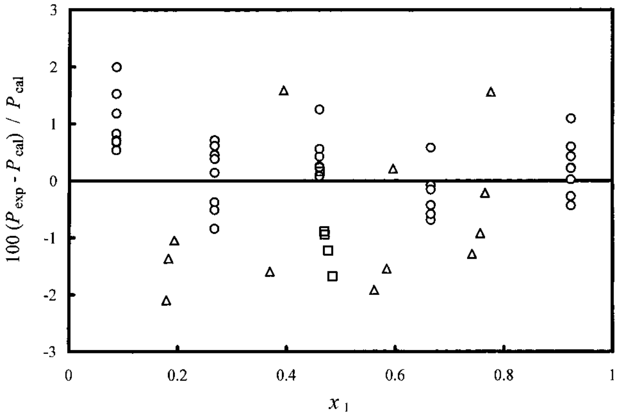

Figure 4. Bubble-point pressure deviation from the PR equation for the binary R-125 + R-134a system: (△) Higuchi; (○) this work; (□) Kleemiss.

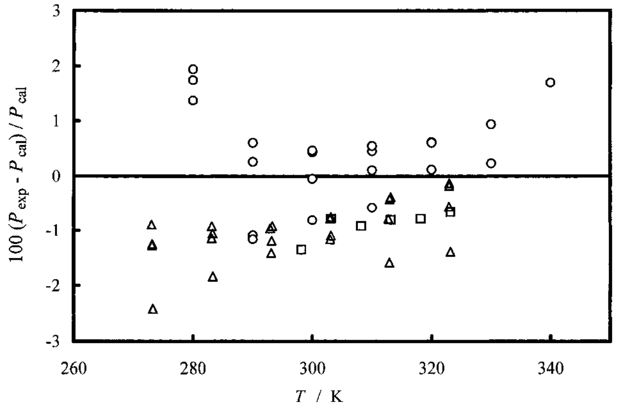

Figure 5. Bubble-point pressure deviation from the PR equation for the ternary R-32 + R-125 + R-134a system: (△) Hihara; (○) this work; (□) Kleemiss.

Fujiwara et al. (1992), by Higashi (1995a), and by Kleemiss et al. (1995). Fujiwara et al. (1992), Higashi (1995b), and Kleemiss et al. (1995) reported also the bubble-point pressures of the binary R-32 + R-125 system. There also exist the data by Kleemiss et al. (1995) and Higuchi and Higashi (1995) reported for the binary R-125 + R-134a system. These existing data were added to the present measured bubble-point pressures so as to optimize the binary interaction parameter of the PR equation. The binary interaction parameter of each binary system has been correlated as a function of temperature, and they are listed in Table 12.

The binary interaction parameter of the PR equation approaches a constant being independent of temperature when the temperature becomes lower. At higher temperatures, however, it departs significantly from the constant value with increasing temperature. For the binary R-32 + R-134a system on which the data are available for a wide temperature range, the binary interaction parameter has been optimized as a nonlinear temperature function, while for the binary R-32 + R-125 and R-125 + R-134a systems it is a linear temperature function since the data availability is very restricted.

The bubble-point pressure deviation from the PR equation for the binary R-32 + R-134a system is shown in Figure 3 where the abscissa is the mole fraction of R-32. Also included in Figure 3 are the data by Fujiwara et al. (1992), by Widiatmo et al. (1994), and by Higashi (1995a). The present bubble-point pressures agree with the data by Widiatmo et al. and by Higashi, while the data by Fujiwara et al. deviate systematically by about 4% from the PR equation and the other reported data. One datum of the present study in Figure 3 which shows deviation greater than 5% is for 60 mass % R-32 at 220 K that corresponds to the absolute deviation of −10.8 kPa. The PR equation reproduces most of the data within ±2% although some data points scatter disperse with rather positive deviation.

The deviation of the bubble-point pressure data for the binary R-125 + R-134a system from the PR equation is illustrated in Figure 4. Most of the present data agree within ±1% with the PR equation, while the data by Higuchi and Higashi (1995) show deviations 1% lower than the calculated bubble-point pressures.

The deviation of our bubble-point pressure data for the ternary R-32 + R-125 + R-134a system from the optimized PR equation which simply accompanies the binary interaction parameters of its corresponding binary systems is illustrated in Figure 5. Also plotted in Figure 5 are the data by Hihara et al. (1995) which exist at three compositions near the binary R-32 + R-134a system and one composition near 33/33/34 mass % R-32 + R-125 + R-134a. Our data except at 280 K show very good agreement with the PR equation, while the data by Hihara et al. (1995) are 1% lower, as an average. Agreement of the measured data with the PR equation within ±2% may reflect a sufficient data representation for the ternary R-32 + R-125 + R-134a system by this model which simply accompanies the binary interaction parameter of its corresponding binary systems. This fact may also reflect the reliability of the optimized binary interaction parameters given in Table 12.

Equation 16 has been introduced to represent the liquid densities of the refrigerant mixtures of the present interest,

$$\ln \frac{v_{\mathrm{m}}}{v_{\mathrm{s,m}}} = A \ln\left(\frac{P + B}{P_{\mathrm{s}} + B}\right) \qquad (16)$$

where v and P are the molar volume and the pressure, respectively. A form of eq 16 was originally proposed by Sato (1981) to represent the compressed-liquid densities of water. Taking advantage of its simple functional form, we have made a modification by introducing the saturated liquid PVT properties into the Sato equation, which then produces eq 16. P_{s} is the bubble-point pressure of the refrigerant mixture, while v_{s} the saturated-liquid molar volume. The coefficients A and B in eq 16 are given as follows:

$$A = -1.04099 + 2.23113T_{\mathrm{R}} - 1.32536T_{\mathrm{R}}^{2} \qquad (17)$$

$$B = -1.25874 \times 10^{5} + 5.68265 \times 10^{5}T_{\mathrm{R}}^{1/3} - 9.51882 \times 10^{5}T_{\mathrm{R}}^{2/3} + 7.02702 \times 10^{5}T_{\mathrm{R}} + 1.93214 \times 10^{5}T_{\mathrm{R}}^{4/3} \qquad (18)$$

Note that the P_{s} value is calculated from the PR equation discussed previously. For the binary R-32 + R-134a and R-125 + R-134a systems the empirical correlations given by eqs 19 and 20, respectively, are somewhat practical to calculate the P_{s} values.

$$P_{\mathrm{s}} = 70.0125 - 14.0117/T_{\mathrm{R}} - 117.473T_{\mathrm{R}} + 66.3508T_{\mathrm{R}}^{2} \quad \text{(for R-32 + R-134a)} \qquad (19)$$

$$P_{\mathrm{s}} = 1 - 4.35068(1 - T_{\mathrm{R}})^{0.23} + 1.88919(1 - T_{\mathrm{R}})^{-0.25} \quad \text{(for R-125 + R-134a)} \qquad (20)$$

with

$$T_{\mathrm{R}} = T/T_{\mathrm{c,m}} \qquad (21)$$

The $T_{\mathrm{c,m}}$ in eqs 17−21 is the critical temperature locus calculated from the mixing rule applied to the modified HBT equation which includes two binary interaction parameters, k_{ij} and l_{ij} given in Table 11. The modified HBT equation is also used to represent the saturated-liquid molar volume of the refrigerant mixtures used in eq 16. The parameters used in the modified HBT equation are also given in Table 10.

k_{ij} is optimized on the basis of the critical temperature data for the binary R-32 + R-134a, R-32 + R-125, and R-125 + R-134a systems reported by Higashi (1995a), Ikeda et al. (1994), and Higashi (1995c). l_{ij} is determined on the basis of the present saturated-liquid densities. In the case of the binary R-32 + R-125 system, l_{ij} has been optimized independently of temperature since the data are available for a restricted temperature range.

The liquid density deviation, including the saturated-liquid and the compressed-liquid ones, of the binary R-32 + R-134a and R-125 + R-134a systems from eq 16 is depicted in Figure 6. As shown in Figure 6, eq 16 represents well the liquid densities of the binary R-125 + R-134a system, while a larger deviation has been observed for the binary R-32 + R-134a system at higher temperatures. This larger deviation is considered due to a less accurate representation of the liquid densities by the modified HBT equation, eq 16. An alternative correlation to represent the saturated-liquid densities of the binary R-32 + R-134a system is that reported by Widiatmo et al. (1995). However, the modified HBT equation is useful to represent the saturated-liquid densities of the ternary R-32 + R-125 + R-134a system because of its mixing rules, as already discussed.

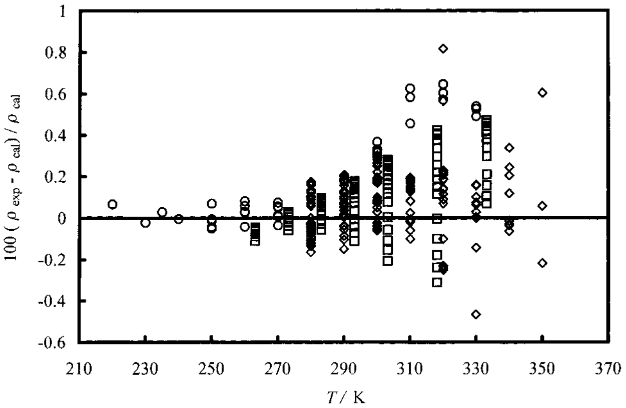

Figure 6. Liquid density deviation from eq 16 for the binary systems: (◇) this work (R-125 + R-134a); (○) this work (R-32 + R-134a); (□) Kleemiss.

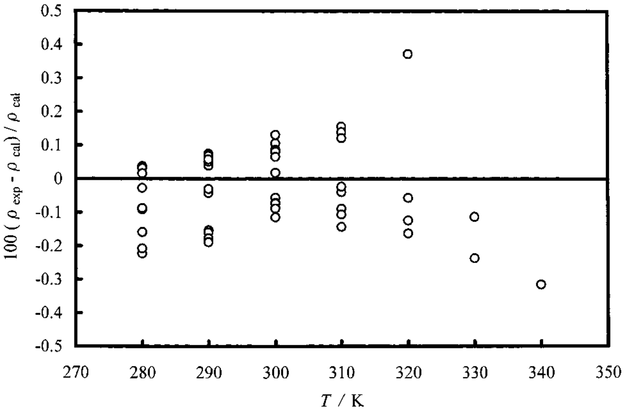

Figure 7. Liquid density deviation from eq 16 for the ternary R-32 + R-125 + R-134a (○) this work.

Figure 7 shows the liquid density deviation for the ternary R-32 + R-125 + R-134a system from eq 16 which includes the saturated-liquid densities calculated from the modified HBT equation. In this case, the modified HBT equation only includes the binary interaction parameters of its corresponding binary systems without any ternary interaction parameter. The deviation in Figure 7 shows a weak temperature dependence, although a sufficient data reproduction has been observed.

Literature Cited

Fujiwara, K.; Momota, H.; Noguchi, M. Vapor-Liquid Equilibria of HFC-32 Mixture (in Japanese). *Proc. Jpn. Symp. Thermophys. Prop., 13th* **1992**, 61−64.

Higashi, Y. Vapor-Liquid Equilibrium, Coexistence Curve and Critical Locus for Binary R-32 + 134a. *Int. J. Thermophys.* **1995a**, *16* (5), 1175−1184.

Higashi, Y. Vapor-Liquid Equilibrium, Coexistence Curve and Critical Locus for Binary R-32 + 125 Mixture. *Proc. Int. Congr. Refrig., 19th* **1995b**, IVa, 297−304.

Higashi, Y. Personal communication, 1995c.

Higuchi, M.; Higashi, Y. Measurement of the Vapor-Liquid Equilibrium for Binary R-125 + 134a Mixture (in Japanese). *Proc. Jpn. Symp. Thermophys. Prop., 16th* **1995**, 5−8.

Hihara, E.; Nakano, M.; Moroyama, N.; Saito, T.; Tanimura, Y. Measurement of Vapor Pressure of Mixture Refrigerant HFC-32 + 125 + 134a (in Japanese). *Proc. Jpn. Joint Conf. Air-cond. Refrig., 29th* **1995**, 29−32.

Ikeda, T.; Kanei, K.; Higashi, Y. Determination of the Critical Locus for Binary R-32 + 125 Mixture (in Japanese). *Proc. Jpn. Symp. Thermophys. Prop., 15th* **1994**, 137−140.

Kleemiss, M. Personal communication, 1995.

Maezawa, Y.; Sato, H.; Watanabe, K. Saturated Liquid Densities of HCFC-123 and HFC-134a, *J. Chem. Eng. Data* **1990**, *35* (3), 225−228.

Maezawa, Y.; Sato, H.; Watanabe, K. Some Correlations for Saturated-Liquid Density of Refrigerant Mixtures (in Japanese) *Trans. JAR* **1993**, *10* (1), 125−133.

Peng, D. Y.; Robinson, D. B. A New Two-Constant Equation. *Ind. Eng. Chem. Fundam.* **1976**, *15* (1), 59.

Piao, C. C.; Sato, H.; Watanabe, K. Thermodynamic Charts and Cycle Reformance of HFC-134a and HFC-152a. *ASHRAE Trans.* **1990**, *96* (Part 1), 132−149.

Qian, Z.-Y.; Nishimura, A.; Sato, H.; Watanabe, K. Compressibility Factors and Virial Coefficients of Difluoromethane (HFC-32) Determined by Burnett Method. *JSME Int. J.* **1993**, *36* (4), 665−670.

Sagawa, T.; Sato, H.; Watanabe, K. Thermodynamic Properties of HFC-125 based on the PVT Measurements. *High Temp.—High Pressures* **1994**, *26*, 193−201.

Sato, H. The Study of the PVT Surface of Vapor and Liquid Water under High Pressures. Ph.D. Dissertation, Keio University, Japan, 1981.

Widiatmo, J. V.; Sato, H.; Watanabe, K. Saturated-Liquid Densities and Bubble-point Pressures of the Binary System HFC-32 + HFC-125. *High Temp.—High Pressures* **1993**, *25*, 677−683.

Widiatmo, J. V.; Sato, H.; Watanabe, K. Saturated-Liquid Densities and Vapor Pressures of 1,1,1-Trifluoroethane and Difluoromethane. *J. Chem. Eng. Data* **1994**, *39* (2), 304−308.

Widiatmo, J. V.; Sato, H.; Watanabe, K. New Predictive Method for the Liquid Densities of HFC Refrigerant Mixtures (in Japanese). *Proc. Jpn. Symp. Thermophys. Prop., 16th* **1995**, 181−184.

Received for review July 9, 1996. Accepted November 18, 1996.[⊗]

JE9602327

[⊗] Abstract published in *Advance ACS Abstracts,* January 15, 1997.